NASA TECHNICAL MEMORANDUM

SELF-ADAPTIVE DIFFERENCE METHOD FOR THE EFFECTIVE SOLUTION OF COMPUTATIONALLY COMPLEX PROBLEMS OF BOUNDARY LAYER THEORY

W. Schönauer, H.-G. Däubler, G. Glotz and J. Grüning

Translation of "Selbststeuernde Differenzenverfahren zur effektiven Lösung von stark rechenintensiven Problemen der Grenzschichttheorie," University of Karlsruhe, Computer Center, Numerical Flow Mechanics Research Division, presented at the DGLR (German Aerospace Society) Annual Convention, 9th., Munich, West Germany, September 14-16, DGLR Paper No. 76-185, pp. 1-20 (A77-16564).

NATIONAL AERONAUTICS AND SPACE ADMINISTRATION
WASHINGTON, DC 20546 JUNE 1986

STANDARD TITLE PAGE

1. Report No.	2. Government Accession No.	3. Recipient's Catalog No.
NASA TM-88440		

4. Title and Subtitle	5. Report Date
SELF-ADAPTIVE DIFFERENCE METHOD FOR THE EFFECTIVE SOLUTION OF COMPUTATIONALLY COMPLEX PROBLEMS OF BOUNDARY LAYER THEORY	June 1986
	6. Performing Organization Code

7. Author(s)	8. Performing Organization Report No.
W. Schoenauer, H.-G. Daeubler, G. Glotz, J. Gruening	
	10. Work Unit No.

9. Performing Organization Name and Address	11. Contract or Grant No.
The Corporate Word, inc. 1102 Arrott Bldg. Pittsburgh, PA 15222	NASW-4006
	13. Type of Report and Period Covered
12. Sponsoring Agency Name and Address National Aeronautics and Space Administration Washington, DC 20546	Translation
	14. Sponsoring Agency Code

15. Supplementary Notes Translation of "Selbststeuernde Differenzenverfahren zur effektiven Loesung von stark rechenintensiven Problemen der Grenzschichttheorie," University of Karlsruhe, Computer Center, Numerical Flow Mechanics Research Division, presented at the DGLR (German Aerospace Society) Annual Convention, 9th, Munich, West Germany, September 14-16, DGLR Paper No. 76-185, pp. 1-20 (A77-16564).

16. Abstract An implicit difference procedure for the solution of equations for a chemically reacting hypersonic boundary layer is described. Difference forms of arbitrary error order in the x and y coordinate plane were used to derive estimates for discretization error. Computational complexity and time were minimized by the use of this difference method and the iteration of the nonlinear boundary layer equations was regulated by discretization error. Velocity and temperature profiles are presented for Mach 20.14 and Mach 18.5; variables are velocity profiles, temperature profiles, mass flow factor, Stanton number, and friction drag coefficient; three figures include numeric data.

17. Key Words (Selected by Author(s))	18. Distribution Statement
Difference methods of optimal error classification, self-adaptive difference methods, numerical solution of hypersonic boundary layer equations, nonstationary boundary layer.	Unlimited

19. Security Classif. (of this report)	20. Security Classif. (of this page)	21. No. of Pages	22. Price
Unclassified	Unclassified	25	

A77-16564 (ORIGINAL)
NASA-HQ 2
N-156,121
N86-26549#

SELF-ADAPTIVE DIFFERENCE METHOD FOR THE EFFECTIVE SOLUTION OF COMPUTATIONALLY COMPLEX PROBLEMS OF BOUNDARY LAYER THEORY

W. Schönauer, H.-G. Däubler, G. Glotz and J. Grüning
Flow mechanics research division
Karlsruhe University computing center

1. BACKGROUND

As a spacecraft re-enters the earth's atmosphere (figure 1), /1* the air in the stagnation point area heats up so intensely that molecular oxygen and nitrogen dissociate and nitric oxide emerges as a significant intermediate compound. Consequently, chemical reactions take place in the air. A five-component air pattern would, for example, include the components N_2, O_2, NO, N and O. The composition is indicated by mass ruptures $w_1 = p_i/p$ for all components i = 1 to N.

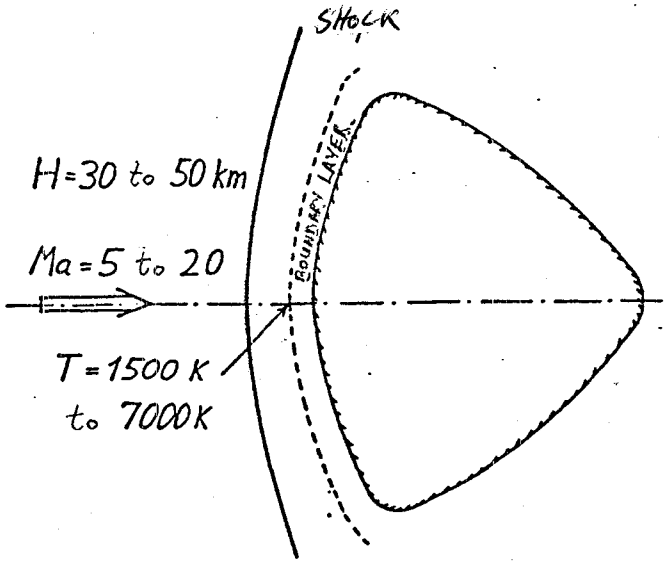

Figure 1. Re-entry.

*Numbers in the margin indicate pagination in the foreign text.

The balanced equations for total mass p, impulse (described by the velocity components u and v), energy (described by temperature T), and individual masses p_i are given to describe the flow. These balanced equations are supplemented by structural equations; for an example of energy current density vector or chemical production densities, see [1]. /2

The resulting equational system is elliptical, i.e., a boundary value problem exists. For technically interesting cases, the calculation expenses for the numerical solution are insurmountable, even with the best computing machines. Therefore, an approximation theory for large Reynolds numbers is used instead, by which the flow is next calculated frictionless, and then transport operations are considered only in the boundary layer. In this way, heat transfer can be calculated on the contour.

2. HYPERSONIC BOUNDARY LAYER EQUATIONS

The resulting boundary layer equations and boundary conditions are given in [1], sections 7 and 8. Figure 2 shows the applicable coordinate system. As a result of the high flight altitude, the Reynolds number lies in the area at which, despite the high velocity, laminar flow exists.

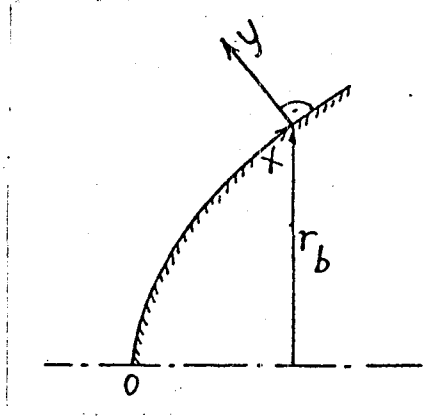

Figure 2. Boundary layer coordinates.

The non-linear differential equations do not have to be given here. The complete system is shortened to operator notation as follows:

$$\left.\begin{array}{l}\text{Equation of continuity}\\ \text{Impulse equation}\\ \text{Energy equation}\\ \text{Component equations of}\\ \text{continuity for i=1 to N}\end{array}\right\} \qquad \vec{P}\,\vec{X} = 0 \; ; \quad \vec{x} = \begin{pmatrix} u \\ v \\ T \\ w_i \end{pmatrix} \tag{1}$$

$\vec{P}\,\vec{x}$ (operator $\vec{P}$ applied to $\vec{x}$) indicates the entire equational system which is ordered so that the right side immediately becomes zero. The first component from $\vec{P}\,\vec{x}$ indicates the equation of continuity, and so forth. One of the component equations of continuity is replaced by the relation /3

$$\sum_{i=1}^{N} w_i - 1 = 0 \tag{2}$$

since the system is otherwise linearly sloped. The system proves itself to be extremely "rigid" as a result of its inherent chemical reaction formula (small changes in the variables change the coefficients significantly). The solution, with help from conventional differential procedures, is very "costly," because the necessary calculation of thermochemical functions for every grid point is extremely expensive to compute.

3. A FAMILY OF DIFFERENCE FORMULAS

To solve the differential equations, we switch from the continuum to a difference grid (figure 3); derivatives are replaced by difference formulas, i.e. piece by piece the solution is represented by polynomials. The first derivatives appearing in the x-direction are replaced by a reversed

difference quotient, for example

$$u_{x,i,k} = \frac{1}{h}\,(u_{i,k} - u_{i-1,k}) + O(h)\ . \qquad (3)$$

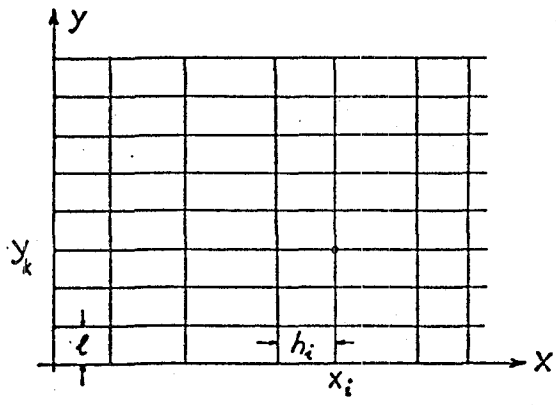

Figure 3. Difference grid.

This formula corresponds to the symbolism in the first line of figure 4: points indicate applicable function values and the circle indicates the place at which the difference quotient is formed. The symbol O(h) means that a discretionary error arises from the order h. By adding further points, we get formulas of a higher order, which form a family of difference formulas. Since lengths that are not equidistant are accepted, we get, in the general case, an error of type $O(\bar{h}^p)$, in which $\bar{h}$ indicates an "average" length.

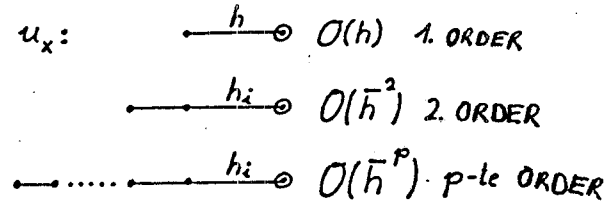

Figure 4. Symbolism for difference formulas in x-direction.

It is important that the discrete error can easily be estimated by the application of a family of difference formulas with help from terms of a higher order of the family. If u_{xD_1} or u_{xD_2} are difference formulas of a higher or lower order of a family and D_1 or D_2 are the accompanying discrete errors, then the following applies, for example, to the derivative u_x:

$$u_x = u_{xD_1} + D_1 = u_{xD_2} + D_2, \text{ from which follows}$$
$$D_1 \simeq u_{xD_2} - y_{xD_1} \quad (+ D_2), \tag{4}$$

i.e., the discrete error D_1 can be estimated by the difference of the difference formulas up to an error D_2. Yet this procedure is only significant as long as $|D_2| < |D_1|$. If $|D_2| > |D_1|$, then the order of the difference formula (polynomial approximation) is "overdrawn." This "practical" estimation is of decisive importance for the controls of the operation, since the "exact" mistakes of type $O(\bar{h}^p)$ are only calculable if the exact solution is known. The coefficients of the difference formulas, like the error formulas derived from them, are calculated by a sub-program with the help of interpolation polonomials directly at the computing machine.

In the y-direction, the derivative u_{yy} is approximated by a family of central, equidistant difference formulas; see figure

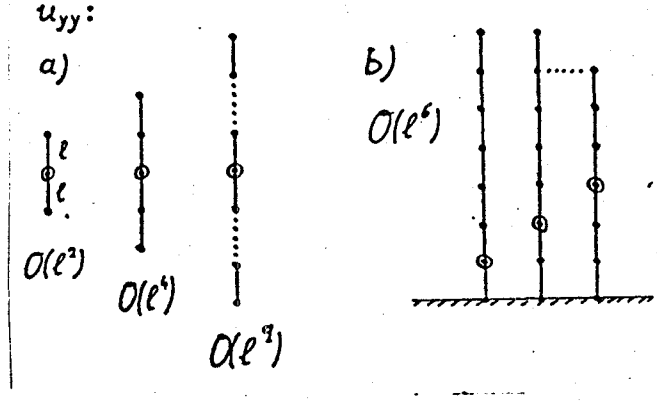

Figure 5. a) central formulas, b) non-central formulas in the margin area.

5a. In the border region, asymmetrical formulas have to be used (see diagram 5b) until the central formulas are applicable. In most cases, we have the formulas of order ℓ^q. Derivatives u_y are likewise approximated; discretionary errors are estimated analogous to equation (4) by the difference from formulas of higher and lower order.

4. DIFFERENCE METHODS

The principle explaining how a non-linear system of differential equations is numerically solved should be illustrated by a simple model equation:

$$P\,u \equiv u_x - a(u)\,u_{yy} = 0\,, \qquad a > o\,. \tag{5}$$

Next, with the help of the Newton Process, a linearized "correction differential equation" is derived in which u is replaced by $u^{v+1} = u^v + \Delta u^{v+1}$, with v as the iteration numerator, which is nevertheless left out in the following equations. From (5) we get

$$(u+\Delta u)_x - a[u+u](u+\Delta u)_{yy} = 0\,.$$

Through development from a to Δu and linearization of the equation in Δu, we get

$$-\Delta u_x + a_u\,u_{yy}\,\Delta u + a\,\Delta u_{yy} = u_x - a\,u_{yy}\,[+0(\Delta u^2)]. \tag{6a}$$

In operational notation, (6a) is shortened to

$$Q\Delta u = Pu\,, \tag{6b}$$

with Q as a linear differential equation operator.

Pu is indicated as the defect, which for an approximate /6

solution u (=u^v) is not equal to zero. Equation (6b) illustrates a quadratic convergent iteration rule, by which Δu is to iterate until it has become "small enough."

Equation (6b) is solved with the difference process, through which the derivatives appearing in Q and P corresponding to figures 4 and 5 are replaced by difference formulas. Figure 6 shows the difference point which thereby arises and which

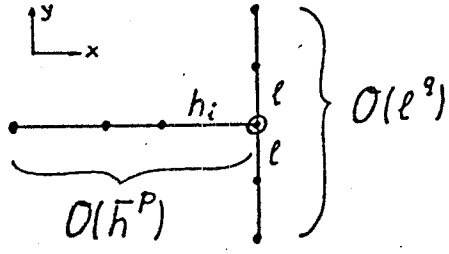

Figure 6. Difference point.

characterizes a dual parametric family of difference methods with the orders p and q as parameters. This implicit method was chosen in order to be able to control the length h_i independent of a stability condition. After the solution for the grid line x_i is calculated, we switch to line x_{i+1}, and so forth. The difference equation for the corrections Δu_D on a grid line reads

$$Q_D \Delta u_D = (Pu)_D + D_x + D_y \ , \qquad (7)$$

with Q_D as the matrix, which arises through the discretion of the operator Q and the related border region with $(Pu)_D$ as the discretionary defect vector. D_x and D_y are the discretionary errors in the x- and y-directions. Solving from (7) to Δu_D (readily accomplished with the help of the Gaus-algorithm) yields

$$\Delta u_D = Q_D^{-1} \left[(Pu)_D \mid + D_x + D_y \right] . \qquad (8)$$

We show equation (8) as an error equation. Up to the broken line, it represents the rule for the calculation of corrections for the Newton-Iteration, from which the defect $(Pu)_D$ is iterated to "zero." The subsequent calculated discretionary errors D_x or D_y become small if $\bar{h}$ or ℓ becomes small. The solution error Δu_{Dy}, determined by the y-discretion, can be estimated by

$$\Delta u_{Dy} = Q_D^{-1} D_y \qquad (9)$$

It is clear that, for effective computation, the three /7
error terminals in the square brackets in (8) must be reasonably balanced. This will next be illustrated in general form.

5. ERROR PROGRESSION

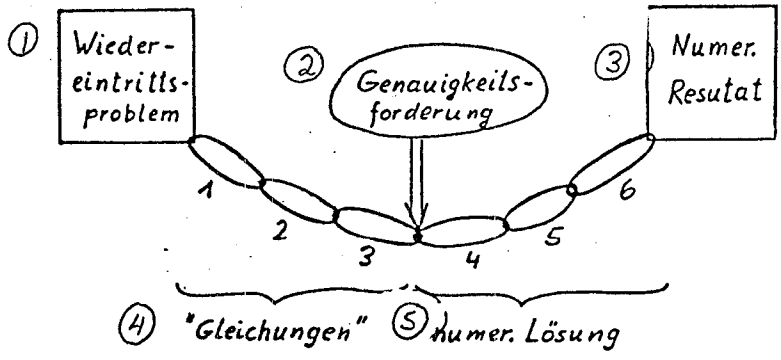

Figure 7. Error progression. Key: 1) Re-entry problem; 2) Accuracy demand; 3) Numerical result; 4) "Equations"; 5) Numerical solution.

In order to progress from the position of a technical problem, for example heat transmission of a re-entering craft, to numerical results, we must run through many error-laden

single steps. The elements of the error progression are:

1. Illustration of a mathematical model (using Navier-Stokes equations).
2. Simplification of the model (using boundary layer equations).
3. Coefficients from thermodynamics (for diffusion, reaction kinetics, etc.)
4. Choice of a numerical solution method.
5. Choice of calculation parameters (lengths).
6 Discontinuance criteria for the iteration.

The accuracy demand "presses" upon the error progression. The greatest error, that is the weakest member of the progression, determines the accuracy. It is not important to calculate with more numerical accuracy than that of the equational model. The calculation costs are minimized if all numerical errors are of equal size and correspond to an established accuracy.

6. TRANSFORMATIONS

In the physical coordinate y, boundary layer thickness and dependent variables change tremendously with running length x; see figure 8a. By applying a modified Falkner-Skan transformation /8

$$\hat{y} = \frac{\rho_a y}{\delta} \quad ; \qquad \delta^2 = \frac{\int_o^x u_a(\xi)d\xi}{u_a^2} \quad ; \qquad (10)$$

$$f = u/u_a \quad ; \qquad g = v\rho_a \delta \quad ,$$

we go from y, u, v, to $\hat{y}$, f, g. As an exception, we might get "similar solutions," which no longer depend on x. In the usual case, the transformation reduces the change in the dependent variables considerably; see figure 8b.

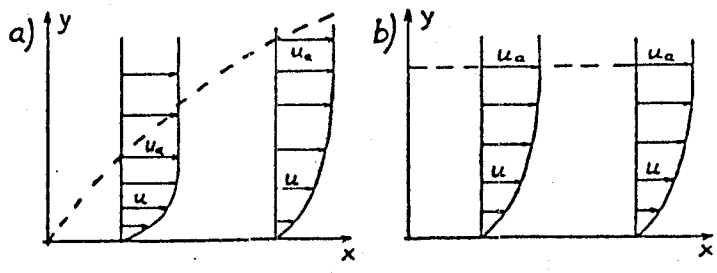

Figure 8. Boundary layer a) without, b) with, similarity transformation.

For the distant method, we are to divide the $\hat{y}$-coordinate equally. Figure 9a shows a boundary layer profile, and figure 9b adds to this the solution error, determined through the /9

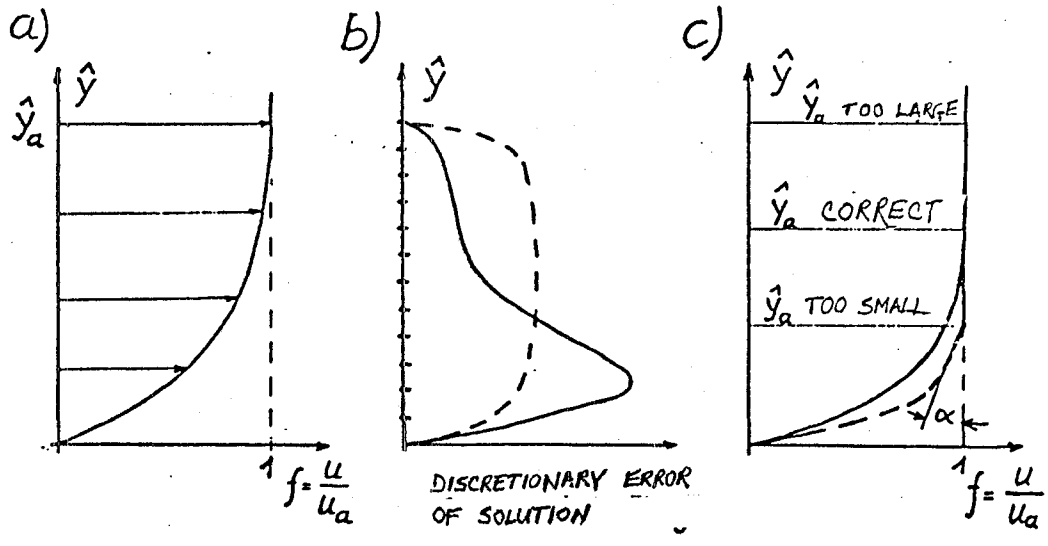

Figure 9. a) Boundary layer profile; b) Error course; c) Asymptotic method.

y-discretion. In the wall region, an error peak appears. By a suitable transformation we can extend the coordinate in the outer region (implicit grid angle) and reach the flattest possible error course. Figure 9c shows the influence of

coordinate $\hat{y}_a$, from which boundary values are determined, on the boundary layer profile. A value for $\hat{y}_a$ that is too small produces large errors; a value for $\hat{y}_a$ that is too large wastes computation time. Therefore, the value of $\hat{y}_a$ is chosen so that tg α corresponds somewhat to the established accuracy of the solution. An implicit grid angle and normalization of the outer coordinates at the value one can be obtained by transition to the numeric coordinate $\bar{y}$ with the following transformation:

$$\hat{y} = \hat{y}_a [c\bar{y} + (1-c)\bar{y}^n] \quad , \tag{11}$$

whereby c and n are so determined that the maximum error is minimized. Figure 10 shows transformation (11) and the grid angle in $\hat{y}$ direction which is then reached.

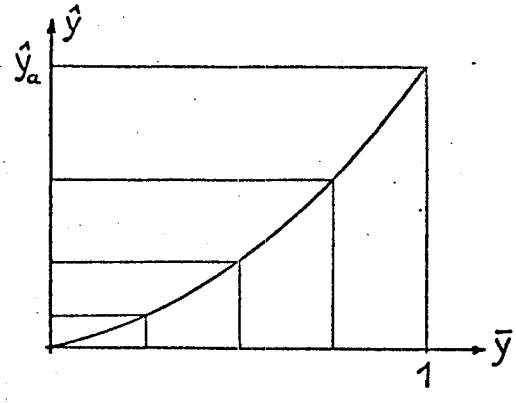

Figure 10. Transformation equation (11).

7. CONTROL IN $\bar{y}$-DIRECTION

The hypersonic boundary layer equations (1) now read in operator notation:

$$\vec{P}\,\vec{x} = 0 \quad , \qquad \vec{x} = \begin{pmatrix} f \\ g \\ T \\ \omega_i \end{pmatrix} \begin{matrix} (u) \\ (v) \\ \\ \rho_i/\rho \end{matrix} \quad . \tag{12}$$

As in equation (6), we also give a Newton-iteration method (in this case at very great expense!)

$$\vec{Q}\ \vec{x} = \vec{P}\ \vec{x}\ , \tag{13}$$

with the linear differential equation operator Q for the correction function $\Delta\vec{x}$. Now we use the difference method /10 with the difference point as in figure 6, and we get, as in (7) and (8), the error equation

$$\Delta\vec{x}_D = A_D^{-1}\ [(\vec{P}\vec{x})_D + \vec{D}_x + \vec{D}_y]\ , \tag{14}$$

which is used to control the calculation.

Figure 11 schematically shows the error determined by the y-discretion, for example temperature T for different orders q depending on length ℓ. The dotted line shows the suitable combinations of ℓ and q in each case. In order to find this

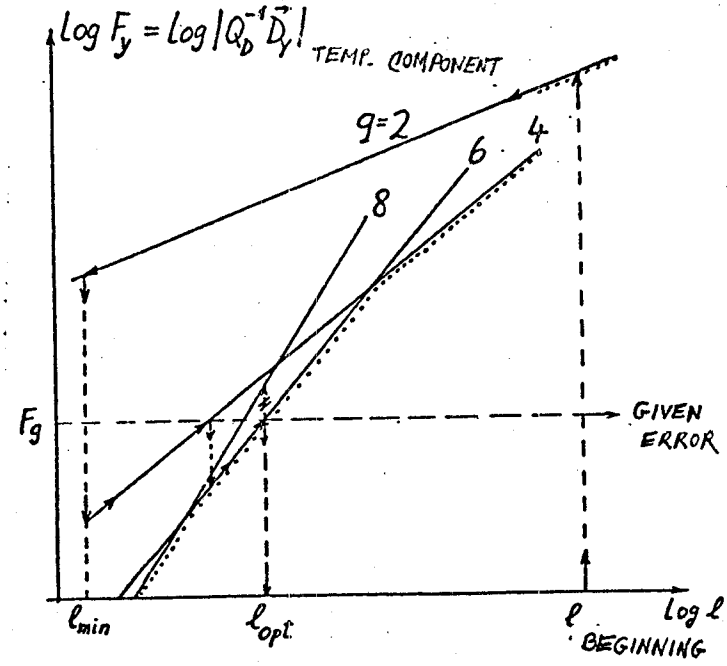

Figure 11: $\vec{Y}$-discretionary error method for solution and determination of ℓ and q.

combination for a given error F_g, the value of ℓ, beginning with q = 2, is determined, and this yields ($\ell \geq \ell_{min}$) as error F_g. Then we go to an order increased by about two (see arrows in figure 11) and so forth until the error grows as the order increases. Then the order would be "overdrawn" so that the last order is best. Figure 11 clearly shows that, for small errors F_g, a high order is best, but for large errors, a lower order is better. This behavior very graphically answers the question "Is a high order better?"

For boundary layer calculation, ℓ,q and $\hat{y}_a$ are determined by iteration of the beginning profile at the stagnation point. For the downstream calculation, ℓ and q remain fixed. This /11 gives the error $\vec{D}_y$ in (14) which is used to control the other errors.

8. ITERATION DISCONTINUANCE AND CONTROL IN x-DIRECTION

The defect $(\vec{P}\vec{x})_D$ in (14) becomes quadratically smaller by successive iterations. An iteration step indicates calculation of a boundary layer profile. The iteration is then broken off as soon as

$$\| (\vec{P}\vec{x})_D \|_{Ko} \approx 0.1 \, \| D_y \|_{Ko} \tag{15}$$

exists, whereby $\| \ \|$ indicates the maximum amount on a line x_i and Ko indicates a component-based comparison (per equation). This makes the iteration error conform to $\vec{D}_y$.

In x-direction, length h_i and order p have to become definite; see figure 6. Length h_i becomes so controlled on every point of x_i that

$$\| \vec{D}_x \|_{Ko} \approx \| \vec{D}_y \|_{Ko} \tag{16}$$

takes effect. Thereby, $\vec{D}_x$ conforms to $\vec{D}_y$. Order p is optimized by comparison with neighboring orders p±1: order p is optimal if the errors of the neighboring orders are larger (figure 12a); it can be increased if, for all components, the growing order error decreases (figure 12b); it must be lowered if, for one component, the error of order p-1 is smaller (polynomial "overdrawn").

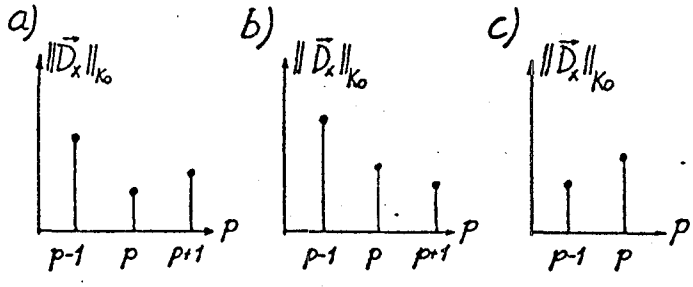

Figure 12. Control of order p.

In order to get good output profiles for iteration, the profiles for position x_i are extrapolated with order p from the preceding profiles. The extrapolation represents a simple predictor. The complete solution method and its application to the hypersonic boundary layer equations are described in [2] - [5]. /12

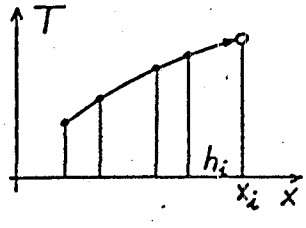

Figure 13. Extrapolation.

9. RESULTS

Results are given for the flow on the so-called AGARD-hyperboloid, figure 14, namely for a typical case of unequal weight (A4) and a case of approximately equal weight (A); see [5]. The profiles for u/u_a as well as T/T_a, in each case at the stagnation point, are given in figure 15. The profiles were calculated with 0.1% accuracy points for temperature T. The temperature profile in case A of approximately equal weight

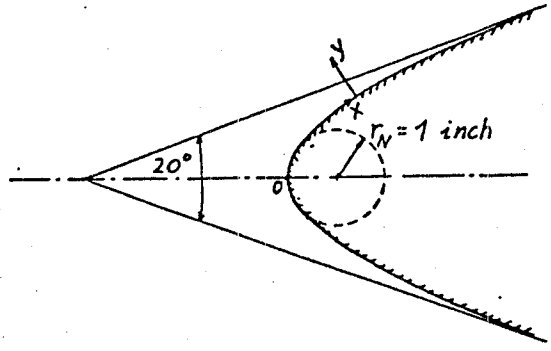

Figure 14. AGARD-Hyperboloid.

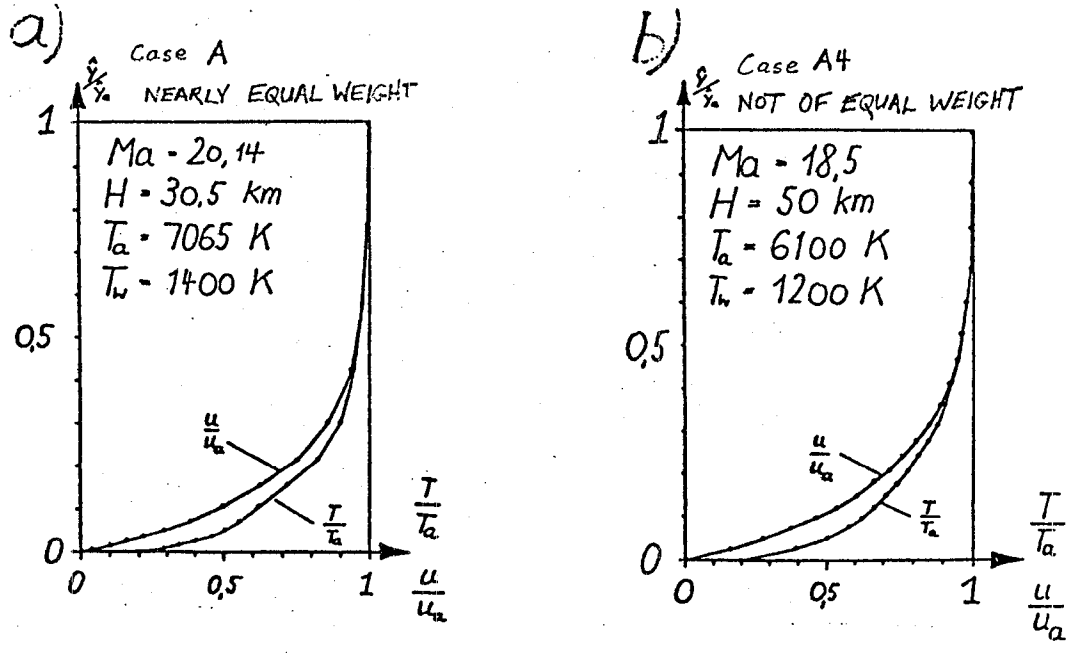

Figure 15: Velocity and temperature profiles for AGARD-cases A and A4 at the stagnation point.

shows a "dent" caused by the chemical reactions. In figure 16, the profiles of mass rupture w_i are given at the stagnation point for the applied 5-component air pattern.

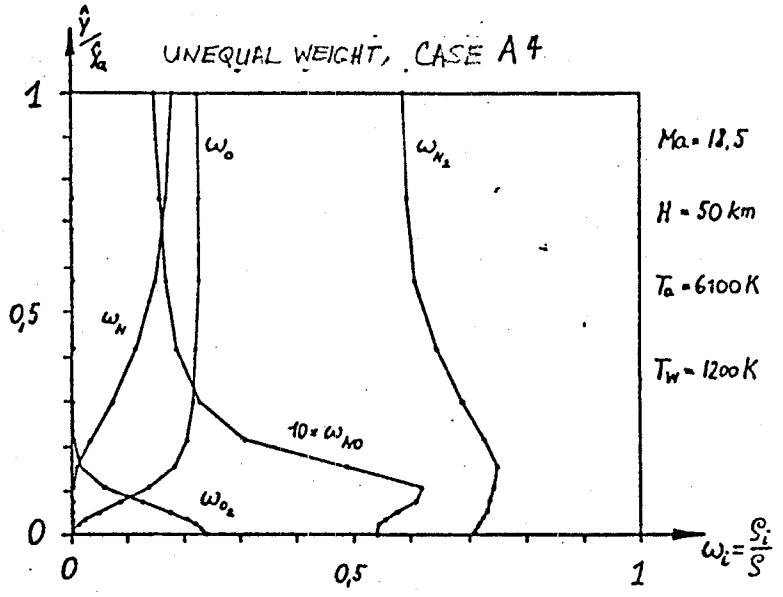

Figure 16. Profile of mass rupture w_i for AGARD-case A4 at the stagnation point.

Figure 17 shows the progress of the Stanton number (heat transmission) and of the friction coefficient along the contour of the AGARD-hyperboloid for cases A and A4 (at 1% accuracy for temperature T).

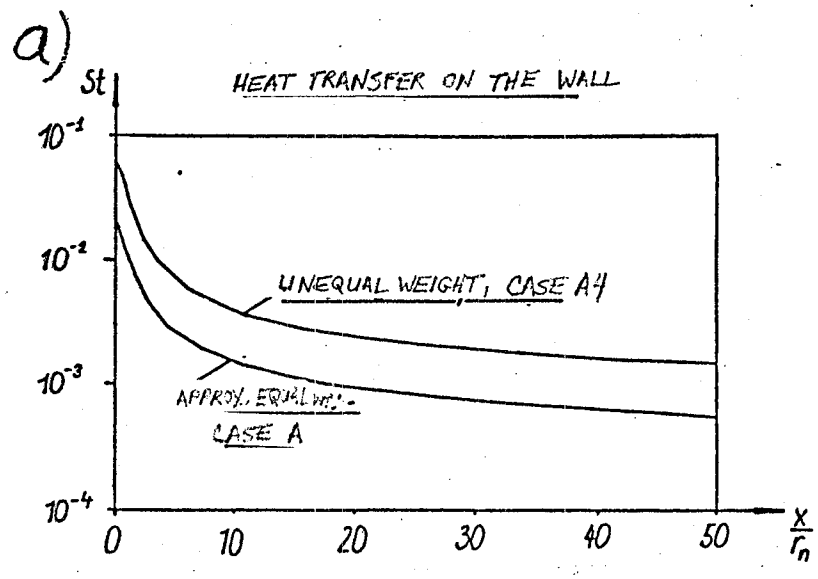

Figure 17a. Progress of Stanton number St along the contour coordinates x for cases A and A4.

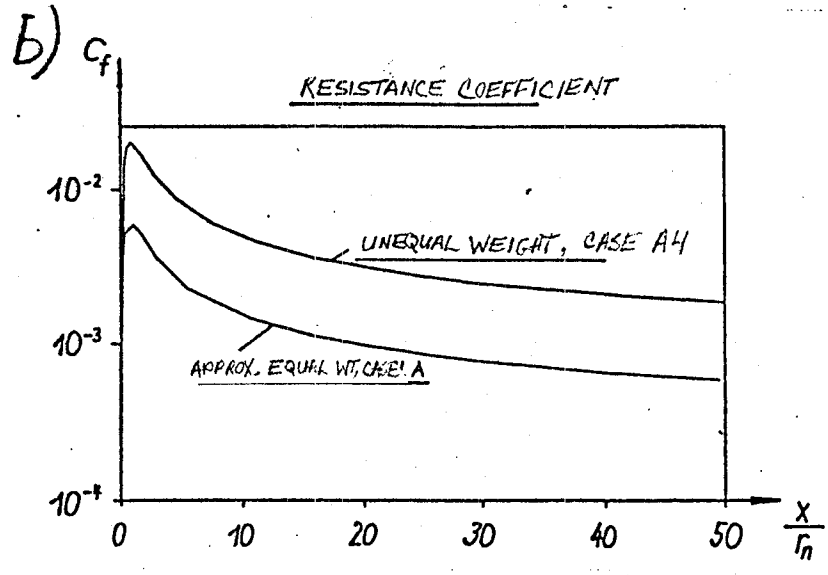

Figure 17b. Progress of friction coefficient c_f along the contour coordinate x for cases A and A4.

The computer program, produced with the support of the Volkswagen Foundation and the Society for Space Research, is available to those interested. It was modularly constructed so

that it can be easily altered for other flow problems or thermodynamic models. Detailed documentation is given in [6]. The calculations were done on the UNIVAC 1108 computer at the computing center of Karlsruhe University.

10. NON-STATIONARY, 3-D, OR TURBULENT BOUNDARY LAYER

The differential equations of the non-stationary hypersonic boundary layer read in operator notation as

$$M \vec{x}_t + \vec{P}\vec{x} = 0 \qquad (16)$$

with $\vec{P}$ and $\vec{x}$ from (12) and a diagonal matrix M. Inclusion of the additional time coordinate t means that, at the discretion in each moment t_j, a complete two-dimensional boundary layer is to be evaluated; figure 18.

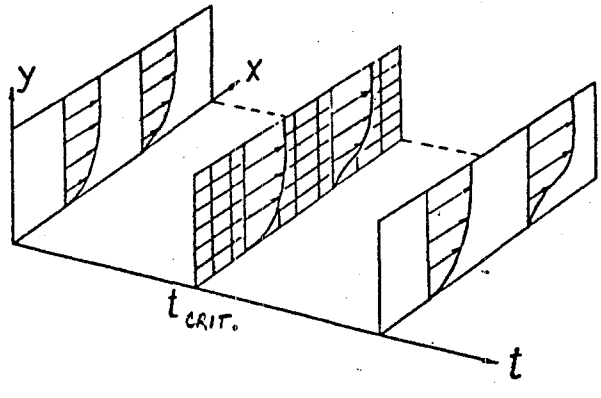

/15

Figure 18. Non-stationary boundary layer.

In the x- and t-directions there is a problem of initial value, and in the y-direction there is a boundary value problem. Accordingly, a completely implicit difference point is used (figure 19) with error orders p, q and r in the x-, y-, and t-directions.

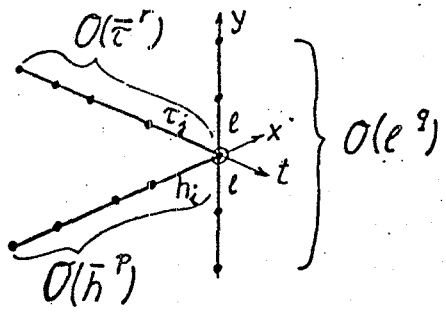

Figure 19. Difference point for non-stationary boundary layer.

The problem of generating an optimal difference grid is solved as follows:

1. For the stagnation point x = 0, time t_{crit}, from which the largest y-discretion error emerges, is determined by given values of ℓ and q.

2. For $t = t_{crit}$, stationary ℓ_{opt}, q_{opt} is determined at the stagnation point; then the stationary boundary layer along length x is solved, and from that lengths h_i are determined and accumulated. Then the x,y-grid is established.

3. The non-stationary equations are solved, and from them time-length τ_j and orders p and r are determined for each instant t_j analogous to section 8. Here the discretion errors are balanced so that

$$\| D_t \| \simeq \| D_x \| \simeq \| D_y \| \qquad (17)$$

applies.

Results from a multitude of examples show that, for /16 chemically reacting boundary layers, the non-stationary terms

play a role only at very large time-gradients (as for the shock tubing method); see [7].

A self-adapting difference method for three-dimensional, incompressible boundary layer equations is being developed. Flow lines (x) and potential lines (y) are chosen as coordinates on the contour, and a similarity transformation is used. Error calculation shows that, by these means and with a relatively rough grid, good accuracy can already be achieved. The difference points are shown in figure 20 with optional error order in all three coordinates.

Until now, these solution methods have only been used for the laminar case. Since the methods are self-adaptive, they adapt easily to turbulent flow; in particular, by error calculation, they aid in finding grid angles which best capture the viscous substratum. But the problem of the turbulent boundary layer so far lies closer to element number 1 of the error progression from figure 7. As long as no reliable field equations for the turbulent flow are given, we cannot expect any exact results completely independent of applicable numbers.

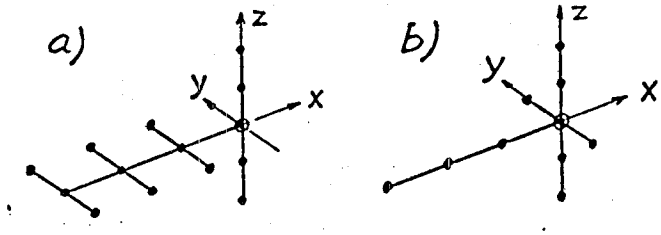

Figure 20. a) Half-implicit b) Fully-implicit, difference point for 3-D.

11. CLOSING COMMENTS

Let's turn back one more time to the two-dimensional hypersonic-boundary layer and look closely at element number 3 of the error progression in figure 7, which should contain the thermodynamic error. Calculation of the thermodynamic coefficients calls for a considerable portion of computing time. On one hand, the numbers do not have to be more exact than the accuracy made possible by thermodynamics. On the other hand, for some small given accuracy we could use a thermodynamic model that is simpler, less exact, and above all less expensive for making calculations. This problem gave rise to the following questions, which are currently being dealt with. /17

1. How do the errors in the thermodynamic coefficients influence boundary layer results (for example, boundary layer profiles, heat transmission)?

2. Which errors are produced by simple thermodynamic models, for example five reactions instead of eighteen reactions; air as a binary gas instead of a 5-component gas, etc.?

Let us, in closing, still ask the question: Are such expensive procedures, as they are described here, really worthwhile? Next, as to computing time: the additional expenditure for error calculation and self-adaptation bring about a large-scale time savings. The expenditure pays off then, where very calculation-intensive problems are presented. Furthermore, because of error monitoring, we immediately get numerically reliable results without having to carry out expensive control calculations. Without self-adaptive methods, it would be nearly impossible to attain, for example, the exact calculation of non-stationary hypersonic boundary layers. Then, as for the programming expense: it is high, but here it is a matter of importance to program modularly. Many of our program building blocks (modules) of incompressible developments were

used for the chemically reacting boundary layer, the most modules of the stationary boundary layer being for the non-stationary, and so forth. If a versatile application is possible by skillful programming of flexible building blocks, i.e., a large part of the programming work is usable for other problems, then the high cost here is worthwhile.

REFERENCES

1. D. Straub, W. Schönauer, A. Schaber, Sui Lin, E. Adams. Stationary laminar hypersonic boundary layer for a rotational hyperboloid at thermo-chemical equilibrium of the air, DLR-inquiry report 72-16 (1972).

2. J. Grüning, W. Schönauer. Investigation of the development of effective solution methods for boundary layer equations, ZAMM 55, pp. T 131-133 (1975).

3. H.-G. Däubler, G. Glotz, J. Grüning, W. Schönauer. Difference methods with self-adaptation of the error classification for the solution of two-dimensional boundary layer equations, ZAMM 56, pp. T 171-174 (1976).

4. W. Schönauer, G. Glotz, J. Grüning, H.-G. Däubler. A variable order self-adaptive difference method for boundary layer equations with application to the chemically reacting boundary layer, Proceedings of the GAMM-Conference on Numerical Methods in Fluid Mechanics, DFVLR, Cologne 1976, published by E. H. Hirschel and W. Geller, pp. 197-208.

5. H.-G. Däubler, W. Schönauer, G. Glotz, J. Grüning. Effective difference methods for the solution of laminar hypersonic boundary layer equations for chemical imbalance, Internal Report Nr. 6/76 of the computing center at Karlsruhe University (1976), in preparation.

6. G. Glotz, W. Schönauer, H.-G. Däubler, J. Grüning. Schedule of the computer program for solution of laminar hypersonic boundary layer equations at chemical imbalance, Internal Report Nr. 5/75 of the computing center of Karlsruhe University (1975).

7. H.-G. Däubler, G. Glotz, W. Schönauer. Numerical solution of the non-stationary, two-dimensional hypersonic boundary layer equations with a self-adaptive difference method, appears in ZAMM 57.

End of Document